

## REFRACTIVITY MEASUREMENTS FROM GROUND CLUTTER USING THE NATIONAL WEATHER RADAR TESTBED PHASED ARRAY RADAR

B. L. Cheong<sup>1,\*</sup>, R. D. Palmer<sup>1</sup>, C. D. Curtis<sup>2,3</sup>, T.-Y. Yu<sup>4</sup>, D. Zrnić<sup>3</sup> and D. Forsyth<sup>3</sup>

<sup>1</sup> School of Meteorology, The University of Oklahoma, Norman, U.S.A.

<sup>2</sup> Cooperative Institute of Mesoscale Meteorological Studies (CIMMS)

<sup>3</sup> NOAA/OAR National Severe Storms Laboratory

<sup>4</sup> School of Electrical and Computer Engineering, The University of Oklahoma, Norman, U.S.A.

### 1. INTRODUCTION

In warm seasons, convective precipitation initiation heavily depends on moisture near the surface [e.g., Dabberdt and Schlatter, 1996; Koch et al., 1997]. A necessary condition for an accurate prediction of convective rainfall is a good forecast of where and when convection will develop. Both prediction and understanding of convection is limited by the lack of high spatial and temporal resolution of water vapor measurements [Weckwerth and Parsons, 2003]. Radiosondes that launch twice a day simply do not supply the measurements at the desired level of temporal and spatial resolution. Near surface measurements were deemed necessary but are expensive to implement on a dense network.

A more attractive approach would be to use some kind of remote sensing technique near the surface. Pioneering work by Fabry et al. [1997] attempted to use ground targets to measure refractivity, which is closely related to humidity. Initial experiments were conducted in Montreal, Canada, demonstrating the potential of the technique [Fabry et al., 1997; Fabry and Creese, 1999]. In addition, extensive experiments were conducted during the International H<sub>2</sub>O Project 2000 (IHOP\_2000) campaign [Fabry and Pettet, 2002; Weckwerth and Parsons, 2003]. The technique estimates refractivity from phase measurements of radar echoes by inversely constructing the refractivity field based on the relationship between refractivity and phase.

Based on this approach [Fabry, 2004], a similar refractivity retrieval algorithm was recently developed at the University of Oklahoma and applied to the Phased Array Radar (PAR), which is the centerpiece of the National Weather Radar Testbed (NWRT) that is operated and maintained by the National Severe Storms Laboratory (NSSL). Here, we will exploit the agile beam steering capability of the PAR system for refractivity retrieval. Extremely short dwell times (down to 180 ms for a 90° coverage) are tested and the results are presented here. If the Multi-Function PAR [MPAR, Weber et al., 2005] concept is to become a reality, rapid acquisition of refractivity fields would be an attractive component of the system.

### 2. NATIONAL WEATHER RADAR TESTBED

The Navy's AN/SPY-1A radar system [Sensi, 1988] has recently been adopted for meteorological research by NSSL. The system is also referred to as the PAR system in the NWRT [Forsyth et al., 2005]. The PAR operates at 3.2 GHz and utilizes an array of 4352 elements and a flexible data acquisition system. Real-time beamforming is used to electronically steer the beam for scanning the atmosphere. In addition, raw time-series data from the PAR can be stored for off-line processing. One of the attractive features of the PAR system is the agile beam steering capability that allows for extremely rapid scanning. In addition, image-smearing effects that are inherent in the standard WSR-88D due to antenna motion are eliminated in the PAR system.

### 3. BASICS OF REFRACTIVE INDEX AND RADIO WAVES

Refractive index,  $n$ , of a medium is defined as the ratio of the speed of light in a vacuum to the speed of light in the medium. For the air near the surface of the earth, this number is typically around 1.003 and changes are on the order of  $10^{-5}$  [Bean and Dutton, 1968]. For convenience, a derived quantity referred to as *refractivity* is used in many scientific studies, and is mathematically formulated as follows

$$N = 10^6(n - 1) \quad (1)$$

Refractivity is related to meteorological parameters as shown below [Bean and Dutton, 1968]

$$N = 77.6 \frac{p}{T} + 3.73 \times 10^5 \frac{e}{T^2} \quad (2)$$

where  $p$  represents the air pressure in millibar (mb),  $T$  represents the absolute air temperature in Kelvin (K) and  $e$  represents the vapor pressure in mb. The first term in equation (2) is proportional to pressure  $p$  and is, therefore, related to the air density. The second term is proportional to vapor pressure  $e$ , which is dominated by moisture. The two terms are often referred to as the *dry* and *wet* terms, respectively. Near the surface of the earth with relatively warm temperatures, most of the spatial variability in  $N$  results from the change in the second term (refer to Figure 1).

Quantitatively, given the pressure and temperature (that tends to be relatively homogeneous) over the radar coverage, humidity is expected to be estimated with reasonable

---

\* Corresponding author address: Boon Leng Cheong, University of Oklahoma, School of Meteorology, 120 David L. Boren Blvd., Rm 4640, Norman, OK 73072-7307; e-mail: boonleng@ou.edu

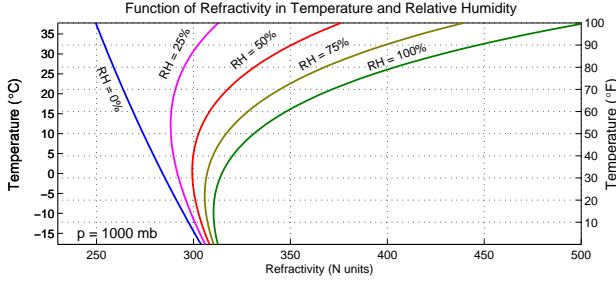


Figure 1: Refractivity  $N$  as a function of temperature  $T$  and relative humidity (derived from  $T$  and  $e$ ). At a surface pressure of 1000 mb and temperature above  $10^{\circ}\text{C}$ , refractive index changes predominantly based on the relative humidity (vapor pressure). As temperature increases,  $N$  becomes more sensitive to the change of  $e$  and thus can be used as a proxy to estimate the water vapor near the surface. This method may be especially useful during warm seasons.

accuracy. At a fixed air pressure, say a typical surface pressure around 1000 mb, refractivity  $N$  becomes a function of  $e$  and  $T$  and is depicted in Figure 1. As temperature increases, refractivity change becomes more sensitive to vapor pressure than to temperature and pressure. One can readily see that vapor pressure  $e$  is the dominant factor that changes the refractivity and, thus, refractivity mapping near the surface can be used as a proxy to estimate the spatial distribution of water vapor near the surface.

#### 4. SUMMARY OF OU'S REFRACTIVITY RETRIEVAL ALGORITHM

Based on the work by Fabry [2004], a separate platform for processing phase measurements to refractivity map is being developed here at the University of Oklahoma (OU). In theory, given that the received phase from stationary targets is an integral function of the refractive index, this quantity can be obtained by performing the derivative operator on both sides of the equation. The received phase is described as follows

$$\phi(r) = \frac{4\pi f}{c} \int_0^r n(\gamma) d\gamma \quad (3)$$

where  $f$  represents the frequency,  $c$  represents the speed of light ( $299,792,458 \text{ m s}^{-1}$ ) and  $r$  is the range. In practice, the radar wavelength that is on the order of cm and  $n \approx 1$ , so the phase wraps many times within a resolution volume depth which makes deriving refractivity directly from a single scan (equation 3) problematic. To mitigate this phase wrapping problem, Fabry et al. [1997] proposed that the change of refractivity between two scans can be obtained instead, i.e.,

$$\begin{aligned} \Delta\phi(r) &= \phi(r, t_1) - \phi(r, t_0) \\ &= \frac{4\pi f}{c} \int_0^r [n(\gamma, t_1) - n(\gamma, t_0)] d\gamma. \end{aligned} \quad (4)$$

If the refractivity field of the reference scan is known, the measurement of the change of refractivity allows us to obtain the absolute refractivity map simply by adding the difference to the reference map. By performing a range derivative in equation (3), it can be shown that

$$\frac{d}{dr} [\phi(r, t_1) - \phi(r, t_0)] = \frac{4\pi f}{c} [n(r, t_1) - n(r, t_0)]. \quad (5)$$

Usually measurement at time  $t_0$  is referred to as the reference, i.e., *reference phase* and *reference refractivity*.

Fortunately for our studies, Oklahoma has a reliable, high-quality network of surface stations, known as the OK Mesonet [Brock et al., 1995]. We will use this network to provide an estimate of the reference refractivity map. Under conditions where the spatial structure of refractivity is not complex, the OK Mesonet allows us to derive an accurate reference refractivity map.

Figure 2 depicts a flowchart of refractivity retrieval algorithm. First, a map of reference phase measurements from the radar, associated with the time of the reference refractivity from OK Mesonet are collected. In general, we would like the structure of the field to be relatively simple, so that the coarse sampling of the Mesonet can be used to produce an accurate reference refractivity map. During normal scanning time, a map of phase measurement is obtained and subsequently used to derive a map of *phase difference* from the reference. Then, regions without *good* ground targets (based on ground clutter coverage and its quality) are masked out to retain only those phase measurements that are useful for refractivity retrieval. A process of spatial interpolation and smoothing is applied to this masked phase-difference map in order to fill the map. By computing radial derivatives (refer to equation (5)) of this smoothed phase-difference map, *refractivity change* can be obtained. Another smoothing is applied to this refractivity change map to reduce the inherent uncertainty in the measurement and derivative operation. Finally, absolute refractivity can be obtained by adding the reference refractivity map to the refractivity change map.

#### 5. EXPERIMENTAL RESULTS

An experiment was conducted on September 28, 2005 using the PAR system for refractivity retrieval. The radar was configured to operate at a pulse repetition time (PRT) of 1 ms. 64 samples were collected for each beam position. The array was set facing north and scanning at an elevation angle of  $0.5^{\circ}$ . The collection parameters resulted in a temporal resolution of approximately 5.76 s. During the collection period, there was a strong low-level northerly wind of approximately  $8 \text{ m s}^{-1}$  causing a light dust storm.

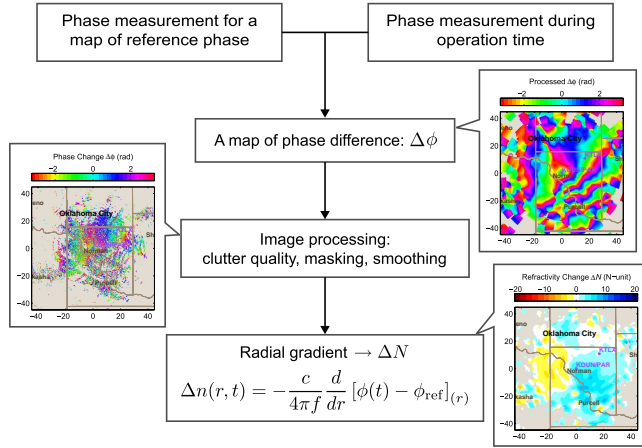
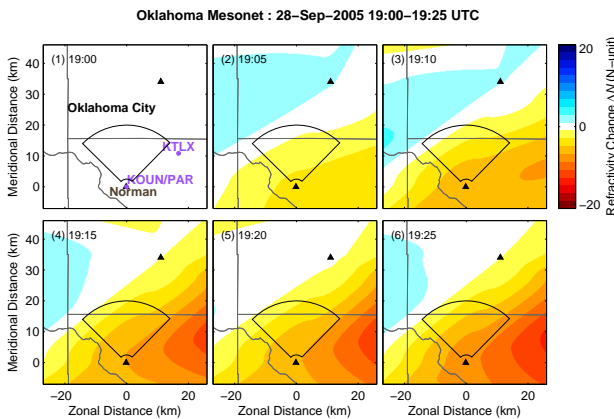


Figure 2: Procedure of refractivity retrieval

Figure 4: Refractivity field derived from surface measurements of the OK Mesonet serves as the ground truth for validation of refractivity retrieval using the NWRT PAR. The solid  $90^\circ$  sector line indicates the area of interest for the PAR-Mesonet comparison.

### 5.1. Validation with OK Mesonet

Since the algorithm estimates the change of refractivity, validation is also conducted on this quantity. By using the refractivity field from the OK Mesonet at the beginning of the experiment as reference, change of refractivity field is derived for comparison. The measurements from the OK Mesonet will be used as ground truth to validate the estimates from the PAR measurements.

Figure 4 shows a sequence of images of refractivity change from the OK Mesonet. Figure 3 shows a similar plot but from the PAR measurements. More images are available but only a subset is shown here. The temporal resolution of the measurements from the OK Mesonet is 5 min, which is the same temporal spacing between each image in the most-left column of Figure 3.

From this comparison between the PAR and the OK Mesonet, we are confident that the refractivity field can be estimated with reasonable accuracy by applying the retrieval algorithm to the S-band PAR. In the next section, rapid scanning using the PAR will be discussed by exploiting the agile beam steering capability of this electronic scanning system.

### 5.2. First Results from the NWRT

In this section, the refractivity fields (derived from 64-pulse dwell) will be used as the ground-truth field. Subsets of contiguous pulses will be extracted from each scan to simulate refractivity fields derived from shorter dwells, which would result in faster scan times. The goal is to investigate refractivity estimates from extremely short dwell-times. Here, 32, 16, 8, 4 and 2-pulse dwells will be tested and compared against the reference (64-pulse dwell). It must be noted that 1-sample dwell was not tested because radial velocity estimation would not be possible and is key for the determination of the usefulness of ground targets. Figure 5 illustrates an example of such a comparison, where the number of pulses is indicated in parenthesis in the upper-left corner. The lower-right panel of Figure 5 shows the quality partitioning of the refractivity estimates.

During the process of deriving the refractivity field, the phase difference map needs to be interpolated and smoothed (refer to Section 4). In the smoothing process, the phase values are first converted into complex form  $\exp(j\phi)$ , with appropriate values set to zero for regions with poor ground targets. Subsequently, the real and imaginary components are processed separately through a weight-and-sum procedure in order to achieve the interpolation and smoothing. Smoothing in this manner avoids the abrupt phase wrapping and difficulties with smoothing over such transitions. While phase of this interpolated-and-smoothed map is used for refractivity calculation, the magnitude is used as our quality metric for refractivity field partitioning. For our statistical comparisons, three partitions have been created to represent regions with high, mid and low quality of estimates.

Different quality of refractivity fields are partitioned and extracted for performance evaluation. Figure 6 shows a plot of the root-mean-squared (RMS) difference (from the 64-point dwell) for various number of samples. As one would expect, for a particular number of samples, the RMS error increases as the quality metric decreases. On the other hand, as the number of samples increases toward 64, the RMS difference decreases. These results show that refractivity retrieval is usable even for a 2-sample dwell time! Note that the RMS difference and its standard deviation at this small number of samples is only 1  $N$ -unit and less than 1- $N$ -unit, respectively, despite the noisy measurements available during the dust storm. A possible explanation for this exceptional performance is that the signal-to-noise (SNR) of the ground tar-

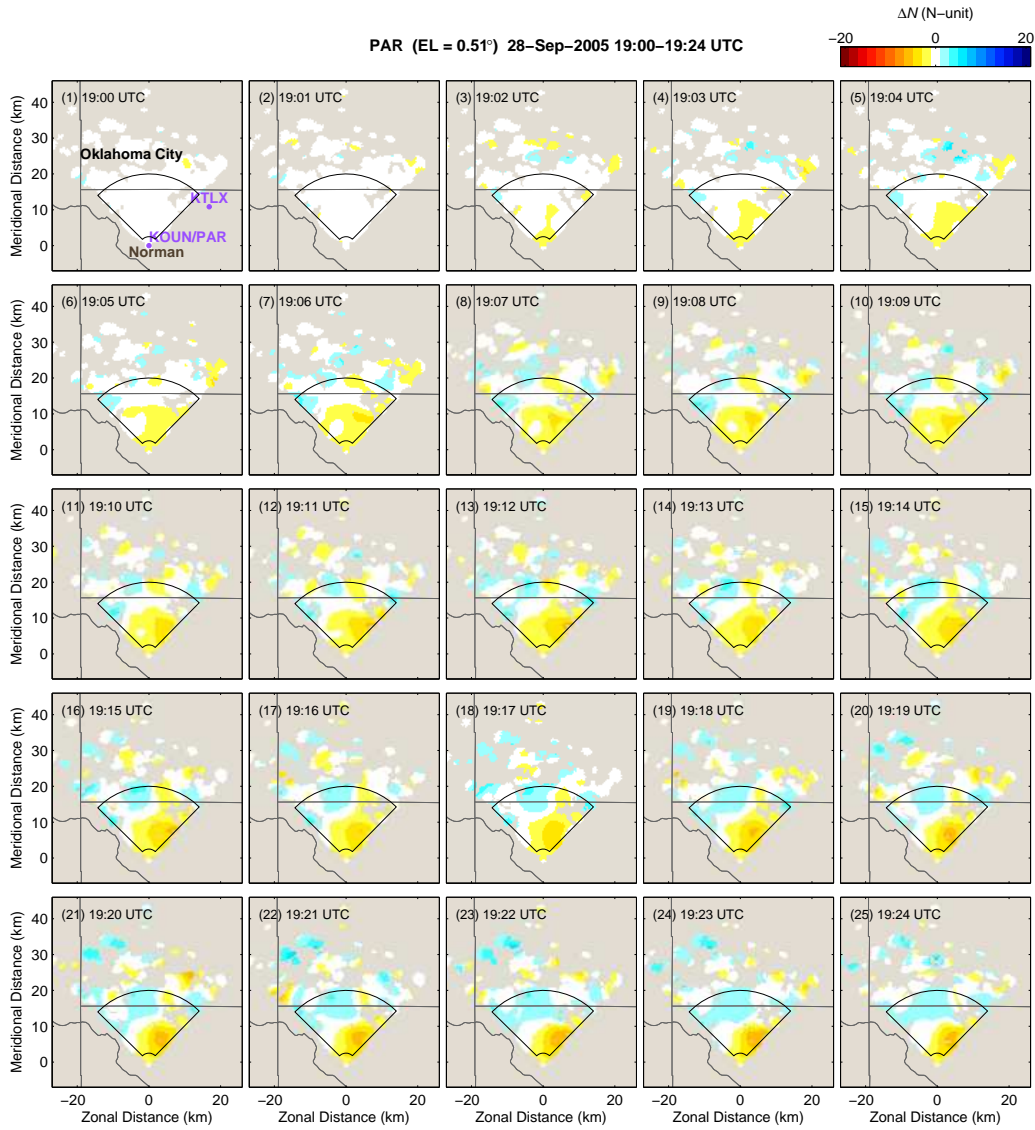


Figure 3: Time history of the refractivity change field retrieved using the PAR measurements shows similar spatial and temporal change from the refractivity fields derived from the OK Mesonet. During this 25-min period, one can see an increase in the refractivity field in the north-western region but a decrease in the region nearer the radar.

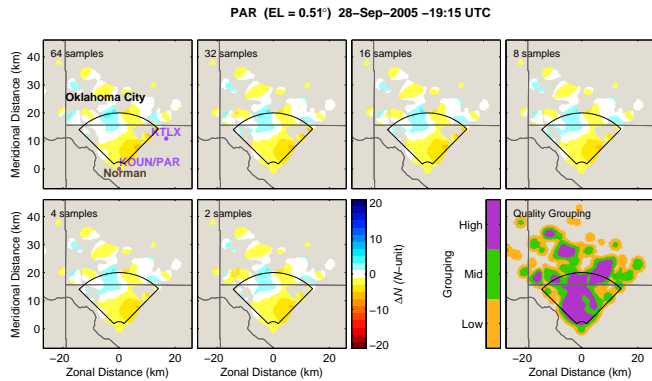


Figure 5: Using the weight-and-sum phase values within the smoothing window, the resulted magnitude is used as a metric to indicate the quality of derived field. Here, the field is partitioned into three regions with different quality index (high, mid and low) for comparison.

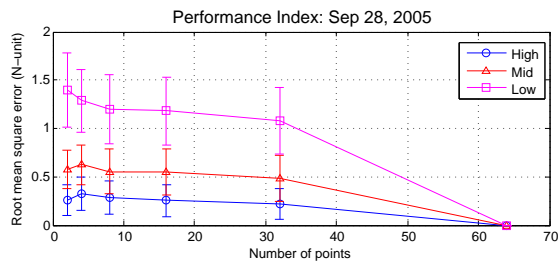


Figure 6: RMS error from Refractivity fields retrieved for various dwell times using the 64-sample case as the reference. The RMS difference of the fields with smaller number of samples are evaluated to compare them against the reference.

gets is sufficiently high. SNR values of 40-60 dB can still easily be found within the coverage and represent the particular targets used for the extraction of refractivity retrieval. As such, even a 2-sample dwell time (with spatial smoothing) suffices for the necessary phase measurements. of the phase estimate with smaller number of samples. This 2-sample dwell with a PRT of 1 ms translates into an extremely rapid 180 ms scan for a 90° coverage.

## 6. CONCLUSIONS

In this article, it has been shown that refractivity retrieval is viable using phase measurements from the S-band PAR of the NWRT. The refractivity fields were compared and validated with surface measurements from the OK Mesonet and were found to be in good agreement. Subsets of the raw samples from the PAR system were extracted to simulate faster scan rates. From this procedure, it has been shown that refractivity retrieval can be accomplished successfully with as little as two samples. If the MPAR system is to become a real-

ity, rapid refractivity retrieval is certainly attractive and would add an important capability to the system.

## References

- Bean, B. R., and E. J. Dutton, 1968: *Radio Meteorology*. Dover Publications.
- Brock, F. V., K. C. Crawford, R. L. Elliott, G. W. Cuperus, S. J. Stadler, H. L. Johnson, and M. D. Eilts, 1995: The Oklahoma Mesonet: a technical overview. *J. Atmos. Oceanic Technol.*, **12**, 5–19.
- Dabberdt, W. F., and T. W. Schlatter, 1996: Research opportunities from emerging atmospheric observing modeling capabilities. *Bull. Amer. Meteor. Soc.*, **77**, 305–323.
- Fabry, F., 2004: Meteorological value of ground target measurements by radar. *J. Atmos. Oceanic Technol.*, **21**(4), 560–573.
- Fabry, F., and C. Creese, 1999: If fine lines fail, try ground targets. in *29th Conf. Radar Meteor.*, pp. 21–23, Montreal, Canada. Amer. Meteor. Soc.
- Fabry, F., C. Frush, I. Zawadzki, and A. Kilambi, 1997: On the extraction of near-surface index of refraction using radar phase measurements from ground targets. *J. Atmos. Oceanic Technol.*, **14**(4), 978–987.
- Fabry, F., and C. Pettet, 2002: A primer to the interpretation of refractivity imagery during IHOP 2002. *IHOP\_2002 Refractivity Manual*.
- Forsyth, D. E., J. F. Kimpel, D. S. Zrnić, R. Ferek, J. F. Heimer, T. McNellis, J. E. Crain, A. M. Shapiro, R. J. Vogt, and W. Benner, 2005: The National Weather Radar Testbed (phased array). in *32nd Conf. Radar Meteor.*, p. CDROM 12R.3, Albuquerque, New Mexico. Amer. Meteor. Soc.
- Koch, S. E., A. Aksakal, and J. T. McQueen, 1997: The influence of mesoscale humidity and evapotranspiration fields on a model forecast of a cold-frontal squall line. *Mon. Weather Rev.*, **125**, 384–409.
- Sensi, Jr., J., 1988: The AEGIS system. in *Aspects of Modern Radars*, pp. 239–277. Artech House.
- Weber, M., J. Cho, J. Flavin, J. Herd, and M. Vai, 2005: Multifunction phased array radar for U.S. civil-sector surveillance needs. in *32nd Conf. Radar Meteor.*, pp. 24–29, Albuquerque, New Mexico. Amer. Meteor. Soc.
- Weckwerth, T. M., and D. B. Parsons, 2003: An overview of the International H<sub>2</sub>O Project (IHOP\_2002). *Bull. Amer. Meteor. Soc.*, **85**(2), 253–277.